© 2014. Published by The Company of Biologists Ltd | Journal of Cell Science (2014) 127, 2483–2492 doi:10.1242/jcs.139923

RESEARCH ARTICLE

# Cytokinesis defines a spatial landmark for hepatocyte polarization and apical lumen formation

Ting Wang[1], Kilangsungla Yanger[2], Ben Z. Stanger[1,2], Doris Cassio[3] and Erfei Bi[1,*]

## ABSTRACT

By definition, all epithelial cells have apical–basal polarity, but it is unclear how epithelial polarity is acquired and how polarized cells engage in tube formation. Here, we show that hepatocyte polarization is linked to cytokinesis using the rat hepatocyte cell line Can 10. Before abscission, polarity markers are delivered to the site of cell division in a strict spatiotemporal order. Immediately after abscission, daughter cells remain attached through a unique disc-shaped structure, which becomes the site for targeted exocytosis, resulting in the formation of a primitive bile canaliculus. Subsequently, oriented cell division and asymmetric cytokinesis occur at the bile canaliculus midpoint, resulting in its equal partitioning into daughter cells. Finally, successive cycles of oriented cell division and asymmetric cytokinesis lead to the formation of a tubular bile canaliculus, which is shared by two rows of hepatocytes. These findings define a novel mechanism for cytokinesis-linked polarization and tube formation, which appears to be broadly conserved in diverse cell types.

**KEY WORDS: Cytokinesis, Par3, Apical tube formation, Exocyst, Hepatocyte, Polarization**

## INTRODUCTION

Epithelial tissue lines body surfaces and cavities and thus plays crucial roles in a variety of functions – including protection, secretion, selective absorption and gas exchange (Datta et al., 2011; Hogan and Kolodziej, 2002; Lubarsky and Krasnow, 2003; Rodríguez-Fraticelli et al., 2011). Epithelial tissue consists of one or more layers of polarized cells that are connected through junctional complexes (tight junctions, adherens junctions, desmosomes and gap junctions), which enables them to act as a structural and functional unit. Epithelial cells are commonly organized into tubes of different sizes and shapes, with their apical domains facing the lumen and their basal domains facing the underlying connective tissue, and several mechanisms that are involved in tube formation have been described (Datta et al., 2011; Hogan and Kolodziej, 2002; Lubarsky and Krasnow, 2003).

The mechanisms underlying epithelial cell polarization and apical lumen formation are not well understood. Studies using 2D cell models, such as Madin-Darby canine kidney (MDCK) cells, suggest that cell–cell adhesion triggers polarization (McCaffrey and Macara, 2012; St Johnston and Ahringer, 2010), whereas emerging evidence from studies involving 3D cultures of MDCK and human intestinal Caco-2 cells suggests that polarization and apical lumen formation are associated with cell division (Jaffe et al., 2008; Schlüter et al., 2009). However, it remains unknown as to whether division-linked polarization defines a general mechanism for epithelial polarization and whether this mechanism can explain physiologically relevant tissue architecture and function.

Hepatocytes, the major parenchymal cells of the liver, are specialized epithelial cells. These cells perform vital functions in humans and other vertebrates – including detoxification, synthesis of serum proteins, metabolism and bile production (Decaens et al., 2008; Wang and Boyer, 2004). Within the liver, hepatocytes are organized into cords in which two rows of cells share a central apical lumen called the bile canaliculus, a specialized tubule into which bile acids and the products of hepatic detoxification are excreted and transported to the small intestine. The basal surfaces of the hepatocytes are adjacent to blood vessels, where serum proteins and hormones that have been produced by the hepatocytes enter the circulation. Thus, the architecture and function of the liver highly depends on hepatocyte polarization and organization. Although other aspects of hepatocyte polarization, such as membrane trafficking and bile canaliculus formation, have been studied extensively in primary hepatocytes and various cell lines (Tuma et al., 1999; Tuma et al., 2001; Wakabayashi et al., 2005; Wang and Boyer, 2004; Zegers and Hoekstra, 1998), the spatiotemporal trigger for the initial polarization of hepatocytes, and the mechanism underlying bile canaliculus formation and tubulogenesis, in the liver remain unknown.

In this study, using the rat hepatocyte cell line Can10 that polarizes and forms bile canaliculi robustly *in vitro* (Treyer and Müsch, 2013; Decaens et al., 2008; Peng et al., 2006), we find that hepatocyte polarization and apical lumen formation are linked to cytokinesis. In addition, we find that oriented cell division is associated with bile canaliculi formation *in vivo*. Our study, together with existing evidence, suggests that cytokinesis-linked polarization is broadly conserved in diverse cell types.

## RESULTS

### Hepatocyte polarization and apical lumen formation are spatially linked to cytokinesis

To determine how hepatocytes become polarized, we observed individual Can 10 cells by time-lapse microscopy. Strikingly, most cells (23 out of 26) did not undergo complete abscission after cytokinesis (Fig. 1A; supplementary material Movie 1). Instead, the daughter cells remained attached and a small bile-canaliculus-like structure appeared at the division site (Fig. 1A, arrow). This structure was clearly observable 2–8 h after cytokinesis by phase-contrast microscopy and became enlarged over time. The canalicular nature of the structure was confirmed

[1]Department of Cell and Developmental Biology, Perelman School of Medicine, University of Pennsylvania, Philadelphia, PA 19104, USA. [2]Gastroenterology Division, Department of Medicine, Perelman School of Medicine, University of Pennsylvania, Philadelphia, PA 19104, USA. [3]INSERM, UMR-S 757, Université Paris-Sud, Orsay, F-91405, France.

*Author for correspondence (ebi@mail.med.upenn.edu)

**Received 2 August 2013; Accepted 27 March 2014**

Journal of Cell Science (2014) 127, 2483–2492 doi:10.1242/jcs.139923

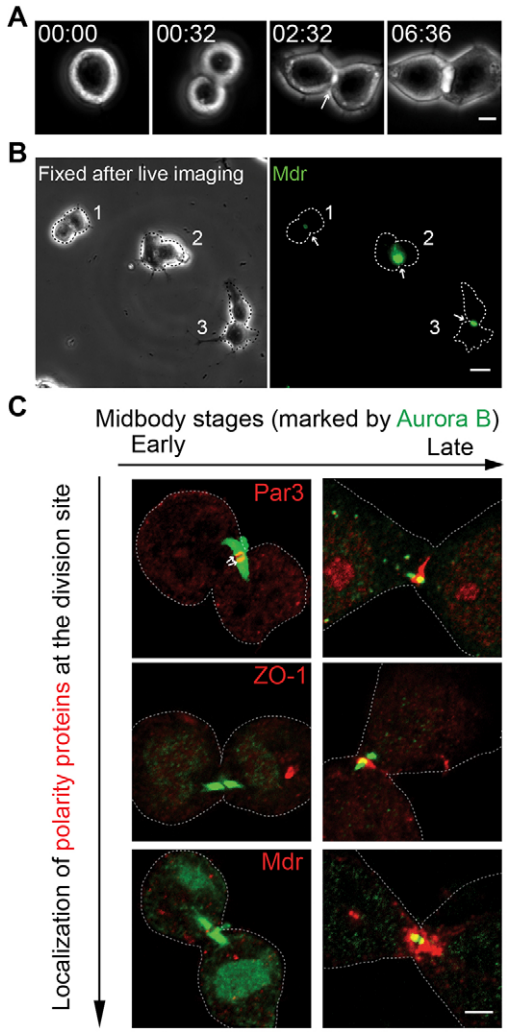


**Fig. 1. Cytokinesis defines a spatial landmark for hepatocyte polarization and bile canaliculus formation.** (A) Time-lapse analysis of cytokinesis and bile canaliculus formation in Can 10 cells. See also supplementary material Movie 1. Time, h:min. (B) Can 10 cells were analyzed by time-lapse microscopy (see also supplementary material Movie 2) and then fixed and stained for Mdr (green, arrow). Dotted lines denote the cell outline. (C) Localization of Par3 (top row, red), ZO-1 (middle row, red) and Mdr (bottom row, red) during different midbody stages (Aurora B, green). Arrows indicate the association between Par3 and Aurora-B-decorated microtubule arrays. Scale bars: 3 μm (A,C); 10 μm (B).

by live-cell imaging, followed by fixation and staining of the imaged cells for Mdr (ABCB1, ATP Binding Cassette, sub-family B, member 1), an authentic bile canaliculus membrane marker (Peng et al., 2006) (Fig. 1B, arrows; supplementary material Movie 2). In a few cells (2 out of 23), the bile canaliculus structure was eventually split into two spheres at the division site, which were subsequently endocytosed (supplementary material Movie 3). Taken together, our data suggest that hepatocyte polarization and apical lumen formation are spatially linked to cytokinesis.

### A polarity regulator, a tight-junction-associated protein and an apical membrane marker localize to the division site in distinct spatiotemporal patterns

To determine how hepatocyte polarization and apical lumen formation are linked to cytokinesis at the molecular level, we monitored the localization of Par3 (also known as Pard3, a key regulator of epithelial cell polarity) (Martin-Belmonte and Mostov, 2008; St Johnston and Ahringer, 2010), ZO-1 (also known as Tjp1, a tight-junction-associated protein) and Mdr during the cell division cycle (Fig. 1C). The late stages of cytokinesis were visualized by staining for Aurora B (also known as Aurkb), a protein kinase that localizes to the central spindle in anaphase and remains on the opposing microtubule arrays that overlap at the midbody before abscission (Delacour-Larose et al., 2004; Gruneberg et al., 2004; Murata-Hori et al., 2002). It became immediately clear that the polarity proteins and bile canaliculus markers localized to the division site in a strict order (Par3 then ZO-1 then Mdr) and with distinct patterns (Fig. 1C). Par3 first localized near the microtubule plus-ends, sandwiching the midbody (Fig. 1C, top left, arrows), and then relocated to the plasma membrane at the division site during the late-midbody stage, which was indicated by the pair of small Aurora B 'bars' (Fig. 1C, top right). Importantly, 93% of the cells ($n$=44) that contained a pair of Aurora B bars showed Par3 localization at the division site (near the midbody or on the plasma membrane). By contrast, ZO-1 did not associate with the microtubule plus-ends during the early-midbody stage (Fig. 1C, middle left) but did localize to the plasma membrane at the division site during the late-midbody stage (Fig. 1C, middle right). However, only 47% of the cells ($n$=58) that contained a pair of Aurora B bars showed this type of localization. Strikingly, Mdr localized near to the minus-ends of the microtubule arrays but not on the plasma membrane at the division site. This pattern of localization was particularly apparent during late-midbody stage (Fig. 1C, bottom right). However, only 25% of the cells ($n$=138) that contained a pair of Aurora B bars showed such localization. Taken together, these data indicate that a key polarity regulator, a tight-junction-associated protein and a bile canaliculus membrane marker are delivered to the division site in distinct spatiotemporal patterns before abscission, and also suggest that hepatocytes begin to polarize at the time of cytokinesis, before lumen formation.

### Assembly and subsequent opening of a disc-shaped tight junction at the division site is accompanied by the emergence of an apical lumen

Our time-lapse analysis indicated that an apical lumen or nascent bile canaliculus formed and enlarged over time at the division site between the divided, yet still attached, daughter cells (Fig. 1A; supplementary material Movie 1). Bile canaliculus formation probably occurs after cytokinesis (defined as the separation of cytoplasm between the daughter cells), as this process was never observed in cells that still contained detectable Aurora B bars. To understand the molecular underpinnings of bile canaliculus formation, we divided the process into three stages – pre-bile-canaliculus, small bile canaliculus and large bile canaliculus – and monitored the key molecular events that are associated with cell polarization and membrane trafficking at each of these stages (Fig. 2). We found that, at the pre-bile-canaliculus stage, the tight-junction-associated protein (ZO-1) and actin filaments (F-actin) colocalized between the two daughter cells as a 'round disc', and the apical vesicles (Mdr) had an intracellular localization that was in close proximity to the disc (Fig. 2A, top). At the small bile canaliculus stage, a clear space formed in the center of the round disc, which is probably caused by the targeted exocytosis of apical vesicles (cf. Fig. 5), resulting in the formation of a ring-like tight junction (Fig. 2A, middle row). This interpretation is supported by the observation that the exocyst (as

Journal of Cell Science (2014) 127, 2483–2492 doi:10.1242/jcs.139923

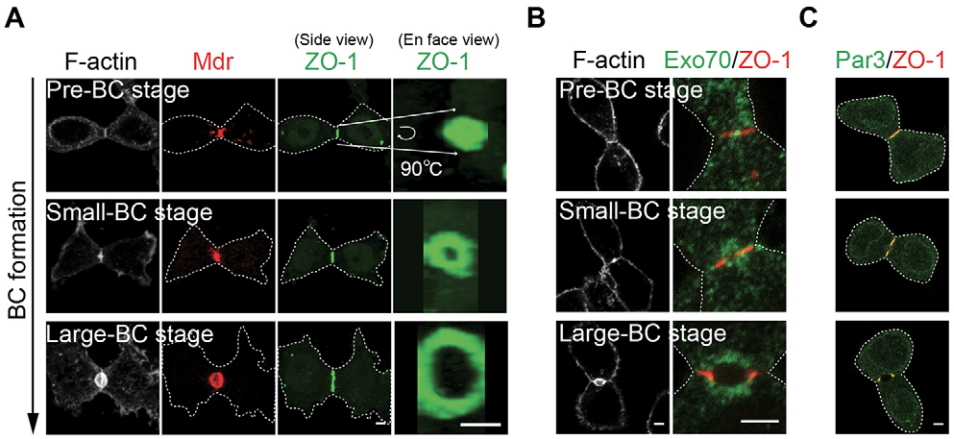


**Fig. 2. Assembly and opening of a disc-shaped tight junction at the division site is associated with *de novo* bile canaliculus formation.** (A) Localization of F-actin (gray), Mdr (red) and ZO-1 (green) during different stages of bile canaliculus (BC) formation in post-cytokinesis cells. All images are snapshots of 3D reconstructions (0.5-μm×8–10 optical slices) at the indicated angles (side or en-face). Pre-bile-canaliculus, small bile canaliculus, and large bile canaliculus stages were defined as those displaying a single line, two lines separated by a short space, and two puncta of ZO-1 signal (side view), respectively. (B) Exo70 (green) localization with respect to ZO-1 (red) and F-actin (gray) during different stages of bile canaliculus formation. (C) Colocalization of Par3 (green) and ZO-1 (red) during different stages of bile canaliculus formation. Dotted lines denote the cell outline. Scale bars: 3 μm.

indicated by its subunit Exo70, also known as Exoc7), a multi-protein complex that is required for vesicle tethering at the plasma membrane (He and Guo, 2009; Novick and Guo, 2002), localized to the center of the tight-junction disc at the pre-bile-canaliculus stage (Fig. 2B, top row) and closely associated with the bile canaliculus membrane at the small bile canaliculus stage (Fig. 2B, middle row). The basic architecture of a large bile canaliculus was very similar to that of a smaller one (Fig. 2A,B; compare bottom and middle rows), with the enlargement of the bile canaliculus, presumably, caused by continued exocytosis (cf. Fig. 5). Basolateral proteins, such as β-catenin, were clearly segregated from the apical proteins during the small bile canaliculus stage and thereafter (data not shown). Strikingly, Par3 displayed perfect colocalization with ZO-1 during each stage of bile canaliculus formation (Fig. 2C), suggesting its involvement in tight-junction assembly, as demonstrated in other epithelial cells (Helfrich et al., 2007; Hirose et al., 2002). Taken together, these data suggest that tight-junction assembly, and targeted exocytosis, at the division site might play a crucial role in bile canaliculus formation.

### Oriented cell division and asymmetric cytokinesis are associated with apical tube formation

Within the liver, the bile canaliculus, which is formed by two adjacent hepatocytes, is part of a tubular bile canaliculus, which is shared by two rows of hepatocytes. To understand how the tubular bile canaliculus arises from the bile canaliculus that is formed at the two-cell stage, we examined the next round of cell division in Can 10 cells that already harbored a bile canaliculus structure. Strikingly, in cells with a pre-existing bile canaliculus and a mitotic spindle, the spindle was oriented, approximately, in parallel to the long axis of the pre-existing bile canaliculus in 71% (±s.d., $n=75$) of the cells (Fig. 3A). In addition, the cleavage furrow, which is perpendicular to the mitotic spindle, ingressed asymmetrically towards the pre-existing bile canaliculus (Fig. 3B). Taken together, these data indicate that oriented cell division and asymmetric cytokinesis are associated with tubular bile canaliculus formation.

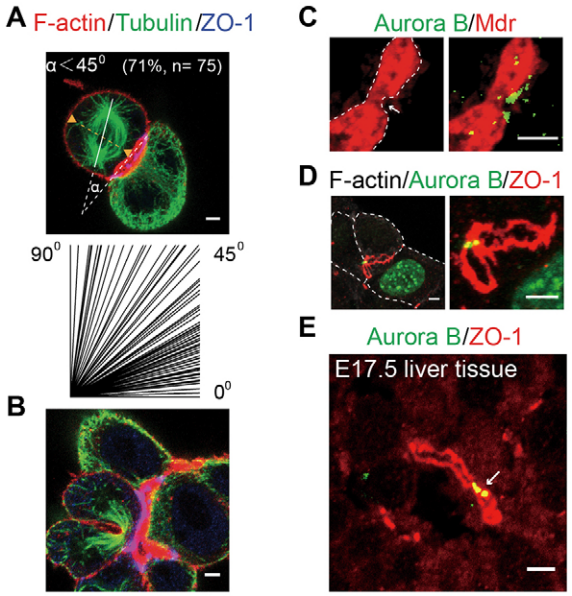


**Fig. 3. Oriented cell division and asymmetric cytokinesis are associated with tubular bile canaliculus formation.** (A,B) Spindle orientation (tubulin, green; each line in the lower panel represents one measurement) (A) and asymmetric furrow ingression (B) with respect to the existing bile canaliculus (F-actin, red; ZO-1, blue) during tubular bile canaliculus formation. (C) A new round of cell division (Aurora B, green) is associated with a constriction point (arrow) on the pre-existing bile canaliculus membrane (Mdr, red). The images are snapshots of 3D reconstructions (0.25-μm×27 optical slices) at specific angles. (D) Tight-junction morphology (ZO-1, red) at the midbody stage (Aurora B, green) during a new round of cell division (see also supplementary material Movie 4). The images are snapshots of a 3D reconstruction (0.45-μm×24 optical slices) at different magnifications. Note that the two sibling hepatocytes involved in the initial bile canaliculus formation do not enter the next cell cycle synchronously (Aurora B is known to decorate interphase nuclei). (E) A new round of cell division (Aurora B, green, arrow) is also associated with the pre-existing bile canaliculus (ZO-1, red) in E17.5 mouse livers. Dotted lines denote the cell outline. Scale bars: 3 μm.

Journal of Cell Science (2014) 127, 2483–2492 doi:10.1242/jcs.139923

Consistent with the conclusion outlined above, we found that in 75%±10 ($n$=126) of the Can 10 cells that contained both a midbody and a bile canaliculus, the midbody was closely associated with the bile canaliculus membrane (Fig. 3C,D; cf. Fig. 4E). Moreover, the bile canaliculus membrane was constricted at the midbody position (Fig. 3C), suggesting that the pre-existing (the 'mother') bile canaliculus is incompletely divided by the contractile actomyosin ring and partitioned into the daughter cells. This suggestion is further supported by our observation that the circle of tight junctions that surround the mother bile canaliculus was also pulled inwards at the division site (Fig. 3D), presumably by the same contractile force, resulting in the formation of two 'lasso-shaped' tight junctions. As new tight junctions are expected to assemble at the division site, followed by bile canaliculus formation within the junctions, at the two-cell stage (Figs 1C; 2A,B), the newly formed junctions and the bile canaliculus at the three-cell, or later, stage must join the old ones to form a more complex network of junctions that surround a single bile canaliculus lumen (supplementary material Movie 4). Taken together, these data suggest that cytokinesis-coupled partitioning of the mother bile canaliculus into the daughter cells, and the further growth of the existing bile canaliculus, might lead to tubular bile canaliculus formation.

To determine whether the tubular bile canaliculus is formed by a similar mechanism *in vivo*, we examined the spatial relationship between cell division and the existing bile canaliculus in liver sections from mice at embryonic day of development (E)16.5 to 17.5, which covers the developmental period for active bile canaliculus biogenesis (Kung et al., 2010; Navarro-Alvarez et al., 2010). Because of the difficulty in distinguishing the true fluorescence signal at the two-cell stage from the background noise in the liver sections (both appeared as small puncta or tiny bands), we could not decipher the mechanism of hepatocyte polarization and bile canaliculus formation at this stage. However, we could detect the association of a pair of Aurora B bars with a tubular bile canaliculus with clarity. We found that whenever an apparent midbody and a tubular bile canaliculus were observed in the same area, they were always closely associated with each other and never separated by any detectable distance (100%, $n$=40) (Fig. 3E). Thus, tubular bile canaliculus formation appears to be dictated by a similar mechanism *in vivo*.

### Par3 is required for tight-junction assembly, and the emergence and expansion of an apical lumen

Our observation that Par3 localizes to the division site before the completion of cytokinesis and to the tight junction during bile canaliculus formation suggests that Par3 might define a molecular link between cytokinesis and apical lumen formation. To examine this possibility, we performed siRNA-mediated knockdown of Par3 (siPar3) and found that the knockdown did not affect overall cell proliferation but did significantly impair bile canaliculus formation (Fig. 4A). The percentage of cells that engaged in bile canaliculus formation was reduced from 80%±2 (±s.d., $n$=1781 from three independent experiments) for the control (siCon) cells to 66%±4 ($n$=1169 from three independent experiments) for the siPar3 cells ($P$=0.0045) (Fig. 4B, left). Par3 knockdown also caused a significant reduction in the average length of each bile canaliculus, reducing from 13±10 µm for the siCon cells (645 bile canaliculi in 1781 cells) to 10±5 µm for the siPar3 cells (318 bile canaliculi in 1169 cells) ($P$<0.001) (Fig. 4B, right). These phenotypes were confirmed by using a different siRNA against Par3 (supplementary material Fig. S1). The remaining bile canaliculi that were observed in the siPar3 cells might reflect an incomplete depletion of Par3 (Fig. 4D; supplementary material Fig. S1D), a preferential requirement of Par3 for bile canaliculus formation but

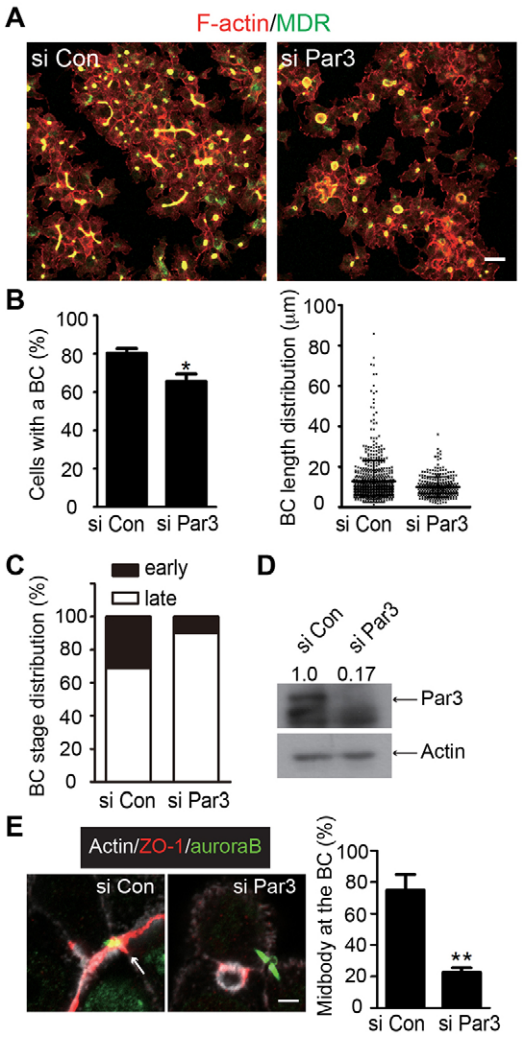


**Fig. 4. Knockdown of Par3 prevents *de novo* bile canaliculus formation and tubular bile canaliculus extension.** (A) Representative images of bile canaliculus formation in the control (si Con) and Par3-knockdown (si Par3) cells. F-actin, red; Mdr, green. (B) The percentage of cells that were engaged in bile canaliculus formation (left) and the bile canaliculus length distribution (right) in the same samples as those shown in A were quantified. Means±s.d. are shown. *$P$<0.005. (C) The distribution of bile canaliculi at early (pre-bile-canaliculus and perhaps small bile canaliculus) and late (large bile canaliculus) stages in the control (si Con) and Par3-knockdown (si Par3) cells. Note that these counts were based on single optical sections of cells that had been stained for ZO-1, Par3 (no Par3 was detected at the tight junctions in the si Par3 cells) and F-actin; thus, it was difficult to distinguish the pre-bile-canaliculus from the small bile canaliculus stage. Therefore, they were grouped together as 'early stage'. However, it is important to note that more than 90% of the 'early-stage' bile canaliculi in the control cells displayed a single line of ZO-1 signal, similar to that at the pre-bile-canaliculus stage, as visualized by using 3D reconstruction. (D) Western blotting indicated that the level of Par3 (relative molecular mass: 150 kD) in the si Par3 cells was reduced to 17% of that in the control cells (the figures are shown across the top of the blot). Actin was used as a loading control. (E) The knockdown of Par3 caused disassociation between the midbody and the pre-existing bile canaliculus. Example images are shown on the left, arrows indicate the association between the midbody and the bile canaliculus. The chart on the right shows the quantification of the cells that retained an association between the midbody and bile canaliculus. **$P$<0.001. Scale bars: 10 µm (A); 3 µm (E).

Journal of Cell Science (2014) 127, 2483–2492 doi:10.1242/jcs.139923

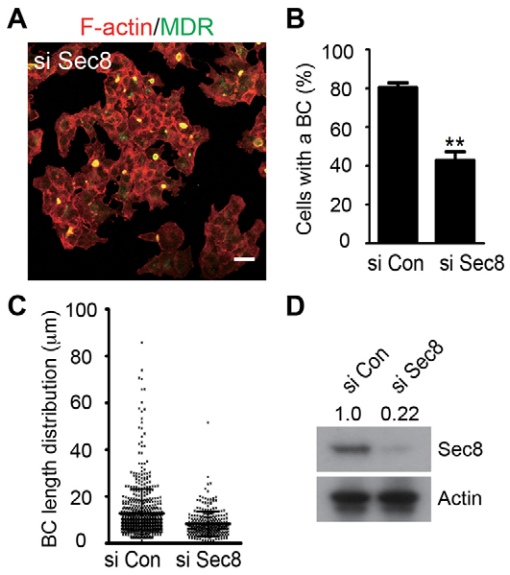


**Fig. 5. The exocyst is required for bile canaliculus formation.** (A) Representative image of bile canaliculus formation in the Sec8-knockdown (si Sec8) cells. F-actin, red; Mdr, green. (B,C) The percentage of cells that were engaged in bile canaliculus formation (B) and bile canaliculus length distribution (C) in the control (the same cells as those shown in Fig. 4A) and si Sec8 cells were quantified. (D) Western blotting indicated that the level of Sec8 (relative molecular mass: 110 kD) in the si Sec8 cells was reduced to 22% of that in the control cells (the figures are shown across the top of the blot). Actin was used as a loading control. Scale bar: 10 μm.

not maintenance (supplementary material Fig. S1E) and/or the involvement of an additional mechanism acting in parallel to Par3. Regardless, these data indicate that Par3 plays a substantial role in bile canaliculus formation, as well as its expansion.

As Par3 displayed perfect colocalization with ZO-1 throughout the process of bile canaliculus formation (Fig. 2C), we thought that Par3 might control bile canaliculus formation by regulating tight-junction assembly. To test this possibility, we examined tight-junction assembly in Par3-knockdown and control cells. Strikingly, tight junctions that were associated with the 'early stage' of bile canaliculus formation (see figure legend for further explanation) were reduced from 31% ($n=109$ cell pairs) in the control cells to 10% ($n=71$) in the siPar3 cells (Fig. 4C). By contrast, the tight junctions that were associated with the later stage of bile canaliculus formation remained high in siPar3 cells (90% versus 69% in the control cells) (supplementary material Fig. S1F). These data indicate that Par3 is required for the *de novo* assembly of a tight junction at the division site and is less crucial for the maintenance of a mature tight junction.

As shown earlier, tubular bile canaliculus formation involved the association between a midbody and a pre-existing bile canaliculus (Fig. 3). Strikingly, such an association was significantly reduced in the siPar3 cells (23%±3, $n=90$), as opposed to the control cells (75%±10, $n=126$) ($P=9.9\times10^{-4}$) (Fig. 4E). This defect might reflect a role of Par3 in spindle positioning, as has been demonstrated in MDCK cells during cyst formation (Hao et al., 2010) (see more in the Discussion).

Taken together, the data described above suggest that Par3 defines a molecular link between cytokinesis and bile canaliculus formation, and that Par3 is required for bile canaliculus formation, as well as its expansion, through the control of tight-junction assembly and spindle orientation.

### The exocyst is required for apical lumen formation

The observation that Exo70 first concentrates at the center of the tight-junction disc and then at the bile canaliculus membrane (Fig. 2B) suggests that targeted exocytosis might drive bile canaliculus formation. To test this possibility, we performed siRNA knockdown of Sec8 (also known as Exoc4), another subunit of the exocyst, which displayed a similar localization profile as Exo70 (cf. Fig. 6B), and examined the effects on bile canaliculus formation. Sec8 was knocked down effectively by the siRNA (siSec8) (Fig. 5D). Bile canaliculus formation was severely defective in the siSec8 cells as compared with that of the control cells (Figs 5A–C and 4A,B). The percentage of cells that engaged in bile canaliculus formation was reduced from 80%±2 (±s.d., $n=1781$ from three independent experiments) for the control (siCon) cells (Fig. 4B, left) to 43%±4 ($n=1357$ from three independent experiments) for the siSec8 cells ($P<0.001$) (Fig. 5B). Sec8 knockdown also caused a significant reduction in the average length of each bile canaliculus – 13±10 μm for the siCon cells (645 bile canaliculi in 1781 cells) and 8±5 μm for the siSec8 cells (295 bile canaliculi in 1357 cells) ($P<0.001$) (Fig. 5C). These phenotypes are clearly more penetrant than those displayed by the siPar3 cells (compare with Figs 5A–C and 4A,B), suggesting that exocytosis might be required not only for bile canaliculus formation but also for its maintenance. Furthermore, siSec8 cells were noticeably more flat and spread out than either the control or the siPar3 cells. Tight junctions formed in the siSec8 cells but they were located at the entire border between neighboring cells (unpublished data), resembling those of MDCK cells in 2D cultures (Gonzalez-Mariscal et al., 1985; McNeil et al., 2006). Taken together, these data indicate that the exocyst plays an important role in the emergence and expansion of a bile canaliculus structure, by promoting apical exocytosis.

### Microtubules are required for the apical localization of the exocyst

To determine how apical exocytosis is targeted to the center of a disc-shaped tight junction in order to drive bile canaliculus formation (Fig. 2), we examined the role of the cytoskeleton in this process, as microtubules and actin filaments are known to mediate long- and short-range vesicle transport in diverse systems, respectively (Bretscher, 2003; Caviston and Holzbaur, 2006). In post-mitotic Can 10 cells, actin filaments were localized throughout the cell cortex but highly enriched in the region surrounding the bile canaliculus (Fig. 6A; supplementary material Fig. S2). Electron microscopy and other studies (Ishii et al., 1991; Tsukada et al., 1995) indicate that there are three distinct populations of actin filaments near to the bile canaliculus – those associated with the tight junctions, those inside the filopodia that are associated with the bile canaliculus membrane and those in an actomyosin (myosin II) network surrounding the bile canaliculus that might be responsible for the contraction and dynamics of the bile canaliculus membrane. By contrast, microtubules are organized into dense networks throughout the cell periphery but did not appear to be selectively enriched at the bile canaliculus region (Fig. 6A; supplementary material Fig. S2) (Decaens et al., 2008). When Can 10 cells were treated with 20 μM latrunculin A (LatA) for 1 h, all actin filaments, except very few in the bile canaliculus region, were disrupted (Fig. 6A; supplementary material Fig. S2). Bile canaliculi remained but their shapes were profoundly altered, changing from the normal ball-shaped bile canaliculi (Fig. 2A) in non-treated cells to a

Journal of Cell Science (2014) 127, 2483–2492 doi:10.1242/jcs.139923

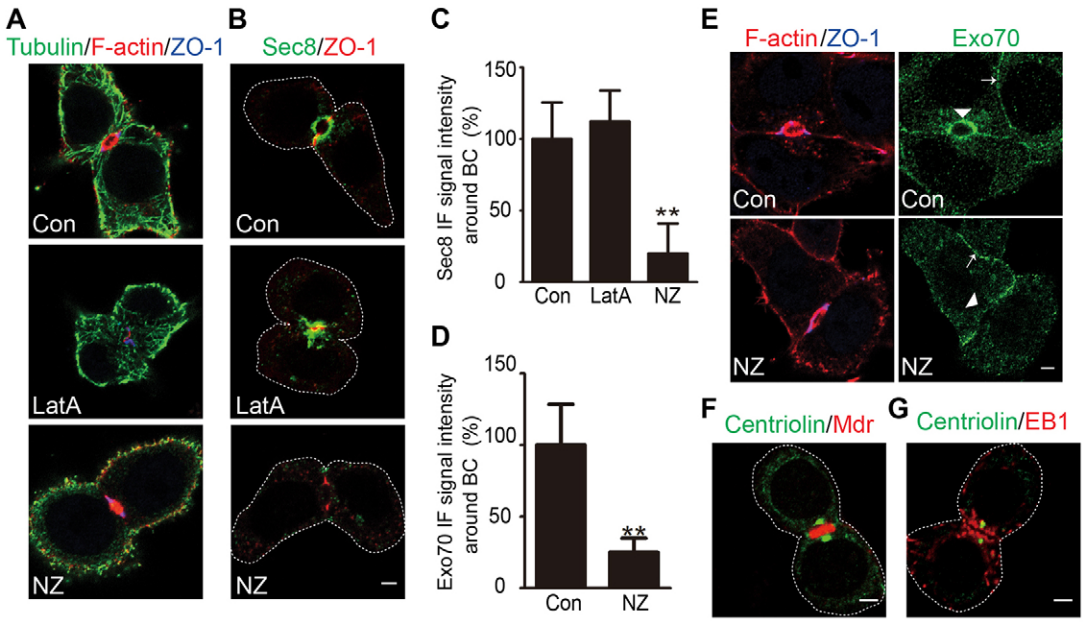


**Fig. 6. Microtubules are specifically required for the apical localization of the exocyst.** (A) The distinct effects of latrunuculin A (LatA) and Nocodazole (NZ) treatments on the actin cytoskeleton (F-actin, red), microtubules (tubulin, green) and bile canaliculus architecture (ZO-1, blue) can be seen. See also supplementary material Figs S2, S3. (B) Distinct effects of LatA and NZ treatments on exocyst (Sec8, green) localization at the bile canaliculus (ZO-1, red). (C) Quantification of the Sec8 immunofluorescence (IF) signal around the bile canaliculus in the control (Con) (set at 100%), LatA- and NZ-treated cells. $^{**}P<0.000001$. (D) Quantification of Exo70 fluorescence signal around the bile canaliculus in the control (Con) (set at 100%) and NZ-treated cells. $^{**}P<0.000001$ (E) NZ treatment specifically disrupts exocyst localization (Exo70, green) at the bile canaliculus but not other cell–cell contact surfaces. F-actin, red; ZO-1, blue. (F) The localization of centrosomes (centriolin, green) with respect to the bile canaliculus membrane (Mdr, red). See also supplementary material Fig. S4. (G) Localization of centrosomes (centriolin, green) and microtubule plus-ends (EB1, red) with respect to the bile canaliculus (inferred by location). Dotted lines denote the cell outline. Scale bars: 3 μm.

variety of convoluted and/or fragmented bile canaliculus structures in cells that had been treated (supplementary material Fig. S3). The exocyst subunit Sec8 was still clustered at the bile canaliculus region but displayed a distribution pattern that, presumably, reflects the underlying change in bile canaliculus shape or structure (Fig. 6B,C) – the Sec8 signal intensity around the bile canaliculus was 100%±26 (±s.d., $n=19$) for the control and 112%±22 ($n=20$) for the LatA-treated cells; $P=0.113$. As expected, the treatment of Can 10 cells with 40 μM Nocodazole for 1 h effectively disrupted microtubules, whereas the actin cytoskeleton and existing bile canaliculi remained intact (Fig. 6A; supplementary material Fig. S2). Remarkably, Sec8 localization at the bile canaliculus region was almost abolished (Fig. 6B,C) – the Sec8 signal intensity around the bile canaliculus was 20%±21 ($n=19$) for the Nocodazole-treated cells; $P=1.31\times10^{-12}$. A similar result was obtained upon staining for the Exo70 exocyst subunit (Fig. 6D) – the Exo70 signal intensity around the bile canaliculus was 100%±28 ($n=20$) for the control and 25%±10 ($n=10$) for the Nocodazole-treated cells; $P=5.25\times10^{-14}$. These data indicate that microtubules are required for exocyst localization, whereas the actin cytoskeleton is required for maintenance of the bile canaliculus architecture.

We also observed that, in addition to its accumulation at the bile canaliculus (Fig. 6E, top, arrowhead), Exo70 localized to other cell–cell contact regions (Fig. 6E, top, arrow). However, treatment with Nocodazole selectively eliminated Exo70 localization at the bile canaliculus but not other locations, suggesting that microtubules are specifically required for the apical localization of the exocyst. These data also imply that microtubules are involved in the polarized transport of apical vesicles during bile canaliculus formation. Because of the high density and complex organization pattern of microtubules in the cortical region of Can 10 cells, it is difficult to visualize a distinct array of microtubules that are associated with the bile canaliculus membrane. To further define the role of microtubules in bile canaliculus formation, we first examined the location of the centrosomes as they are found to be near the apical membrane in some other epithelial cells and are thought to play a role in apical lumen formation, although the underlying mechanism remains unknown (Feldman and Priess, 2012; Rodríguez-Fraticelli et al., 2012). We found that at the pre-bile-canaliculus stage, the centrosomes – as indicated by immunostaining of centriolin, a centrosomal protein that binds specifically to mother centrioles (Gromley et al., 2005) – were localized near to the disc-shaped tight junctions in some cells (supplementary material Fig. S4, top). At the small and large bile canaliculus stages, the centrosomes were, invariably, close to the bile canaliculus structure (supplementary material Fig. S4, middle and bottom; Fig. 6F). These data suggest that, after cytokinesis, the centrosomes must migrate from the spindle poles to the cell division site in order to orchestrate other cellular functions, such as bile canaliculus formation. These data are also consistent with the previously reported finding that γ-tubulin, another component of the centrosomes, is also localized near to the tubular bile canaliculus membrane (Decaens et al., 2008). EB1 (also known as Mapre1), a protein that tracks the plus-ends of dynamic microtubules (Akhmanova and Steinmetz, 2010; Tirnauer and Bierer, 2000), was distributed throughout the cell cortex but was also noticeably enriched near to the bile canaliculus membrane (Fig. 6G). Taken together, these data suggest that an array of

Journal of Cell Science (2014) 127, 2483–2492 doi:10.1242/jcs.139923

microtubules, which originate from the nearby centrosomes, is engaged in exocyst-mediated apical exocytosis to drive bile canaliculus formation.

## DISCUSSION

### Cytokinesis defines a spatial landmark for the emergence of hepatocyte polarity and apical lumen formation

Based on this study, we propose that cytokinesis defines a spatial landmark for hepatocyte polarization and bile canaliculus formation. Our 'cytokinesis-landmark model' (Fig. 7A) posits that, during the terminal phase of cytokinesis, the key polarity regulator Par3 and the tight-junction-associated protein ZO-1 are delivered to the division site sequentially before the completion of cytokinesis, presumably in preparation for subsequent bile canaliculus formation. Centrosomes are then instructed to migrate close to the disc-shaped tight junctions between the daughter cells. After cytokinesis, microtubules, which are likely to have originated from the nearby centrosomes, are specifically required for exocyst localization at the bile canaliculus membrane and are, presumably, involved in the targeted exocytosis of apical vesicles in order to drive bile canaliculus emergence and expansion. While this manuscript was in revision, *de novo* bile canaliculus formation was also reported to occur at the site of abscission in HepG2 cells (Slim et al., 2013). Thus, our 'cytokinesis-landmark model' applies to both rat and human hepatocytes.

With this conceptual framework established (Fig. 7A), major mechanistic questions regarding hepatocyte polarization and bile canaliculus formation can be formulated and addressed in the future using the Can 10 model. For example, we have shown that Par3 localizes to the division site before the completion of cytokinesis and is required for tight-junction assembly and bile canaliculus formation after cytokinesis. Thus, Par3 is ideally positioned to convey the spatial cue from the cytokinesis machinery to enable cell polarization and bile canaliculus formation at the correct time and place. However, it remains unknown as to how Par3 is delivered to the division site and how it regulates tight-junction assembly at the molecular level. According to the cytokinesis-landmark model (Fig. 7A), the centrosomes must migrate from the spindle poles to a region proximal to the bile canaliculus in order to nucleate microtubules that guide exocyst-dependent exocytosis. However, it is also unknown how centrosome migration occurs, how microtubules interact with the exocyst or exocyst-decorated apical vesicles and which Rab GTPase(s) and motor proteins are involved in apical exocytosis.

Does cytokinesis-linked bile canaliculus formation occur at the two-cell stage *in vivo*? For technical reasons (outlined in the Results), we could not decipher the mechanism of cell polarization and bile canaliculus formation at the two-cell stage by using embryonic liver sections and light microscopy methods. However, an electron microscopy study of developing rat livers clearly indicates that tight junctions, with or without an associated bile canaliculus, are detected (at the earliest) on day 13 (the gestation period is 21 days for rats) and are restricted to the contact site between two apposing cells (Wood, 1965), which is strikingly similar to what was observed in Can 10 cells at the two-cell stage. The electron microscopy study also indicates that tight-junction assembly precedes bile canaliculus formation *in vivo*, as observed in Can 10 cells *in vitro*. The apposing cells in the electron microscopy study are likely to be the progeny of a cell division, because, if cell–cell contact were the only trigger for tight-junction assembly and bile canaliculus formation, most of the hepatocytes in a row should be able to develop these structures with two different neighbors at the same time, which is, apparently, not the case (Wood, 1965).

How do hepatocytes find the center of their contact surface to initiate polarization and bile canaliculus formation? This is a fundamental question regarding the geometry of hepatocyte polarization. According to our 'cytokinesis-landmark model', the site of bile canaliculus formation is the site of cell division, which is automatically centered between the daughter cells during cytokinesis, thus solving the geometry problem. Because of its cell-autonomous nature, the cytokinesis-linked polarization mechanism could provide a highly efficient means of bile canaliculus formation during liver development and regeneration.

### Oriented cell division and asymmetric cytokinesis are involved in apical tube formation

In the liver, a tubular bile canaliculus is always sandwiched by neighboring hepatocytes. It remains completely unknown how the tubular bile canaliculus evolves from a round or ovoid bile canaliculus that forms at the two-cell stage. Based on this study, we propose a 'divide-and-grow' model for tubular bile canaliculus formation, which posits that oriented cell division results in the incomplete 'division' and partitioning of the mother bile canaliculus into two daughter cells, and further 'growth' of the bile canaliculus in the daughter cells, which is driven by continued exocytosis, leads to tubular bile canaliculus formation (Fig. 7B). After the first division, the two daughter cells often enter the next cell cycle asynchronously, attesting to their cytoplasmic separation. One daughter cell undergoes the next round of division before the other. The division is oriented with the spindle in parallel to the long axis of the existing bile canaliculus. The division is also asymmetric, presumably due to the association of the contractile ring with the bile canaliculus membrane. Asymmetric furrowing during cell division has been frequently observed *in vivo* for many cell types, including epithelial cells due to their asymmetric attachment to the extracellular matrix (ECM) or neighboring cells (Founounou et al., 2013; Guillot and Lecuit, 2013; Herszterg et al., 2013; Maddox et al., 2007). This oriented division and asymmetric cytokinesis results in the partitioning of the mother bile canaliculus into the two daughter cells. The midbody is associated with the bile canaliculus membrane, and the centrosomes migrate towards the bile canaliculus structure. Similar to the two-cell stage, the centrosomes nucleate microtubules to guide exocyst-dependent apical exocytosis to drive bile canaliculus growth in both daughter cells, as indicated by the localization of the exocyst subunits Exo70 and Sec8 on the bile canaliculus membrane at the three-cell, or later, stage (unpublished data). The daughter cell that undergoes the next round of division after the other will also undergo oriented cell division and asymmetric cytokinesis, as the first daughter does, and contribute to the overall expansion of the shared bile canaliculus along the spindle axis. Repeated oriented divisions along the same axis will lead to two rows of hepatocytes that share a central tubular bile canaliculus with centrosomes located next to the bile canaliculus membrane. This is exactly the pattern of organization that was observed in Can 10 cells using the antibody against Mdr to visualize the tubular bile canaliculus and antibodies against centriolin (unpublished data) or γ-tubulin (Decaens et al., 2008) to visualize the centrosomes. Similar to Can 10 cells, the midbody is always tightly associated with the bile canaliculus membrane in developing livers (shown here). In

Journal of Cell Science (2014) 127, 2483–2492 doi:10.1242/jcs.139923

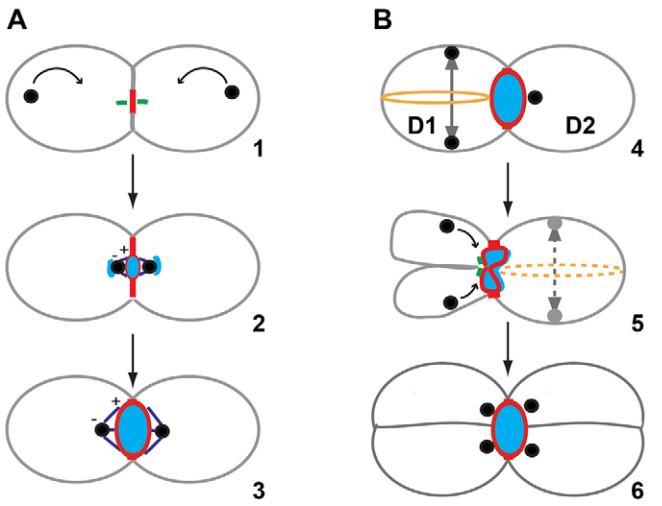


**Fig. 7. Models for hepatocyte polarization and bile canaliculus formation.** (A) Cytokinesis landmark model for hepatocyte polarization and bile canaliculus emergence. During the terminal phase of cytokinesis (represented by microtubule arrays at the midbody stage, green, step1), the key polarity regulator Par3 (red) and the tight-junction-associated protein ZO-1 (red) are delivered to the division site sequentially before the completion of cytokinesis. Centrosomes (black circles) are instructed to migrate (black arrows) close to the disc-shaped tight junctions between the daughter cells. After cytokinesis, microtubules (purple lines with marked + and − ends) (steps 2 and 3) are specifically required for exocyst localization at the bile canaliculus membrane (blue oval) and are, presumably, involved in the targeted exocytosis of apical vesicles (blue lines near the centrosomes; step2) to drive bile canaliculus emergence (step 2) and expansion (step 3). (B) Divide-and-grow model for tubular bile canaliculus formation. Oriented cell division results in the incomplete 'division' and partitioning of the mother bile canaliculus into two daughter cells, and further expansion of the bile canaliculus in the daughter cells, which is driven by continued exocytosis, leads to tubular bile canaliculus formation. After the first division, one daughter (D1) undergoes the next round of division before the other (D2; step 4). The division is oriented with the spindle (the solid line with a double-ended arrow) in parallel to the long axis of the existing bile canaliculus (step 4). The division is also asymmetric (step 5), presumably, due to the association of the contractile ring (step 4, brown circle) with the bile canaliculus membrane. This oriented division and asymmetric cytokinesis results in the partitioning of the mother bile canaliculus into the two daughter cells (step 5). The midbody (indicated by the microtubule arrays) is associated with the bile canaliculus membrane and the centrosomes migrate towards the bile canaliculus structure. The centrosomes nucleate microtubules to guide exocyst-dependent apical exocytosis to drive bile canaliculus growth in both daughter cells. The other daughter cell (D2) will also undergo oriented cell division and asymmetric cytokinesis (step 5, dashed spindle and contractile ring), contributing to the overall expansion of the shared bile canaliculus. Repeated oriented divisions in the same direction leads to two rows of hepatocytes that share a central tubular bile canaliculus with centrosomes located next to the bile canaliculus membrane (step 6).

regenerating livers, the cleavage furrow of a dividing hepatocyte has also been found to be associated with a bile canaliculus in 28% of the cells examined (Bartles and Hubbard, 1986). These observations suggest that tubular bile canaliculus formation might employ the same mechanism *in vitro* and *in vivo*. However, a recent paper reports that, in regenerating mouse livers, weaned rat livers, and HepG2 cells, the spindle axis is largely perpendicular to the bile canaliculus lumen, such that cell division results in asymmetric inheritance of the existing bile canaliculus by the daughter cells (Slim et al., 2013). The authors hypothesize that this mode of oriented cell division, coupled with *de novo* bile canaliculus formation at the site of abscission and further elongation and fusion of individual bile canaliculi, leads to the formation of a complex bile canaliculus network, as seen previously in primary hepatocytes that had been cultured at a high density, sandwiched between two layers of collagen or other ECM (Fu et al., 2010; Fu et al., 2011). Taking these observations together, it is possible that both modes of oriented cell division are involved in bile canaliculus biogenesis *in vivo*. During early liver development, the parallel spindle-axis mode might be preferentially used to generate a tubular bile canaliculus, whereas, during later liver development or regeneration, the perpendicular spindle-axis mode might be preferentially used to build a complex bile canaliculus network.

How spindle orientation is controlled during tubular bile canaliculus formation remains unknown. Par3 is required for oriented cell division during cyst formation by MDCK cells (Hao et al., 2010). It is thought to act by controlling atypical protein kinase C (aPKC, a component of the Par3–Par6–aPKC polarity complex) localization to the apical membrane, which phosphorylates LGN (also known as GPSM2) and results in its dissociation from the apical membrane, thereby inactivating the Gαi–LGN/Pins–NuMA system that is essential for the anchoring of spindle poles to the cell cortex. The serine/threonine kinase Par1 (also known as MARK1) is also known to regulate spindle orientation in epithelial cells through pathways involving RhoA, LGN–NuMA, and the astral microtubules (Cohen et al., 2004; Lázaro-Diéguez et al., 2013). In Can 10 cells, siRNA knockdown of Par3 greatly reduced tubular bile canaliculus formation (Fig. 4A,B) and the association of the midbody with the existing bile canaliculus membrane (Fig. 4E). Both phenotypes are consistent with a role of Par3 in spindle orientation. However, in contrast with MDCK cells, aPKC is not localized to the apical membrane, instead, it colocalizes with Par3 at the tight junctions for the duration of bile canaliculus formation (unpublished data). Thus, how Par3 controls spindle orientation in Can 10 cells requires further investigation. It will also be interesting to determine whether, and how, Par1 is involved in controlling spindle orientation in Can 10 cells.

### Coupling of division to polarization and apical lumen formation appears to be broadly conserved in diverse polarization systems

Accumulating evidence suggests that the coupling of division to polarization and apical lumen formation goes beyond the hepatocyte. When MDCK cells are embedded in ECM, the polarity protein Crumbs 3 (also known as CRB3) is delivered to the division site during cytokinesis, and an apical lumen is formed between the daughter cells after the first division (Schlüter et al., 2009). During cyst formation by the human intestinal Caco-2 cells in 3D cultures, aPKC is localized to the division site during cytokinesis and an apical lumen forms there at the two-cell stage (Jaffe et al., 2008). In a remarkably similar way to Can 10, spindle orientation and asymmetric cytokinesis (the cleavage furrow ingresses from the basal to the apical surface) play crucial roles in cyst formation by the Caco-2 cells (Jaffe et al., 2008). In addition, the midbody is closely associated with the apical membrane (Jaffe et al., 2008). Similar spindle orientation and asymmetric cytokinesis are also observed in the crypt proliferative zone of mouse small intestine during normal tissue renewal (Fleming et al., 2007). Thus, oriented cell division and asymmetric cytokinesis might define a general mechanism for epithelial cell polarization and apical tube formation.

The coupling of division to polarization and apical domain formation also goes beyond epithelial cells. During neural tube formation in zebrafish, neuronal progenitors undergo mirror symmetric cell division. Par3 localizes to the cleavage furrow during cytokinesis and is then partitioned equally to the divided, yet still attached, daughter cells. Subsequently, an apical lumen (a part of the neural tube) is formed at the division site, sandwiched by Par3 in both daughter cells (Tawk et al., 2007). In *Drosophila*, following cytokinesis by a neuronal precursor cell, the first neurite or apical pole, an indicator of the emergence of neuronal polarity, is formed at the Par3-decorated division site (Pollarolo et al., 2011). Thus, Par3 might communicate the spatial signal from division to polarization in cell types ranging from hepatocytes to neurons.

Spatial coupling of division to polarization also exists in fungal cells. In the budding yeast *Saccharomyces cerevisiae*, the division site specifies the location for the next round of polarization or budding (equivalent to apical domain formation) (Bi and Park, 2012). Strikingly, budding can occur repetitively with the previous division site in the apiculate yeast *Saccharomycodes ludwigii* (Streiblova et al., 1964), akin to the Can 10, and other, cells described above. In the rod-shaped fission yeast *Schizosaccharomyces pombe*, immediately after cytokinesis, polarized cell growth always occurs at the old end first (the division site that was formed one or two generations ago) and then at both the old and new ends (the new end is generated during the last cell division) (Martin and Chang, 2005). These observations suggest that molecular memory exists at the previous division sites, which signals where to initiate polarization and cell growth. Taken together, the spatial coupling of division to polarization and apical domain formation appears to be broadly conserved in diverse polarization systems.

## MATERIALS AND METHODS

### Cell cultures and animals

Can 10 cells were cultured in Coon's modified F-12 medium (Sigma) with 5% fetal bovine serum (Gibco). Mice were maintained in a pathogen-free environment. For timed pregnancies, the morning of the vaginal plug was designated day 0.5, and embryos were collected at indicated stages.

### Antibodies and chemicals

The mouse monoclonal antibody (clone c219) against Mdr was purchased from Signet. Rabbit antibodies against Par3 and Aurora B, and a rat antibody against α-tubulin were purchased from Abcam. Mouse and rabbit antibodies against ZO-1 were purchased from Invitrogen. A mouse antibody against Aurora B was purchased from BD Biosciences. Mouse monoclonal antibodies against Exo70 and Sec8 were kindly provided by Wei Guo (University of Pennsylvania, Philadelphia, USA) and Shu-Chan Hsu (Rutgers University, Piscataway, USA). A rabbit antibody against actin was purchased from Sigma. All the fluorescence-labeled secondary antibodies and phalloidin were purchased from Invitrogen. Latrunculin A and Nocodazole were purchased from Wako Pure Chemical Industries and Acros Organics, respectively.

### siRNA knockdown

Silencer® Select Pre-Designed siRNAs against rat Par3 (s135864) and Sec8 (s138195) and the Silencer® Select Negative Control No.1 siRNA were purchased from Invitrogen. The cells were transfected with Lipofectamine RNAiMAX reagent (Invitrogen) following the reverse the manufacturer's reverse transfection protocol. After 48 h, the knockdown efficiency was assessed by western blotting.

### Immunofluorescence and microscopy

Cells were cultured on 35-mm collagen-coated glass-bottomed dishes and then fixed with 4% paraformaldehyde for indirect immunofluorescence or staining with other fluorescence-labeled probes. For staining of Mdr, cells were permeabilized with acetone for 2 min at 4℃. For other antibodies, the cells were permeabilized with 0.25% Triton X-100. Embryonic liver tissues were rinsed in PBS and fixed in $Zn^{2+}$-buffered formalin (Polysciences), embedded in paraffin and cut into sections of 5–8-µm thickness. Sections were incubated in R-buffer A (Electron Microscopy Sciences) for antigen retrieval at 120℃ using a Pickcell 2100 antigen retrieval system. Sections were then rinsed in PBS and blocked with 2% donkey serum for 1 h. After incubating with various antibodies, the cell culture dishes, and the tissue slides, were imaged using the Zeiss LSM710 confocal microscope with a 20× objective lens or 63× oil immersion lens. For phase-contrast time-lapse microscopy, cells were imaged 4 h after passage by using a DeltaVision deconvolution microscope with a 40× lens in a $CO_2$ environment chamber. For the cells that were analyzed by time-lapse imaging and Mdr staining (Fig. 1B), the locations of the cells were marked before time-lapse analysis. After fixation and Mdr staining, the same cells were found and imaged by fluorescence microscopy.

### Image processing and analysis

All images were processed and quantified using the Fiji software (Schindelin et al., 2012). For the quantification of the bile canaliculus length, the longest diameter of round-shaped canaliculi and the longest, and often curved, length of tubular-shaped canaliculi were measured. For quantifying the number of cells that were engaged in bile canaliculus formation, any cell with an apparent bile canaliculus membrane was considered positive.

### Statistical analysis

All data represent the mean±standard deviation (s.d.). Statistical analysis was performed using two-sided Student's *t*-tests.

#### Acknowledgements

We thank Wei Guo, Shu-Chan Hsu, Stephen Doxsey (University of Massachusetts Medical School, Worcester, USA) and Michael Lampson (University of Pennsylvania, Philadelphia, USA) for providing antibodies; Shelly Berger, Rebecca Wells and Ken Zaret (University of Pennsylvania, Philadelphia, USA) for using their tissue-culture facilities; Andrea Stout (University of Pennsylvania, Philadelphia, USA) for imaging assistance; Chenghua Yang (University of Pennsylvania, Philadelphia, USA) for technical assistance; and Amin Ghabrial and Rebecca Wells (University of Pennsylvania, Philadelphia, USA) and the members of the Bi laboratory for discussions.

#### Competing interests

The authors declare no competing interests.

#### Author contributions

T.W. and E.B. designed experiments, analyzed the data and wrote the manuscript, T.W. also performed the experiments. K.Y. and B.Z.S. provided the mouse liver sections and guidance for immunostaining the sections, and helped manuscript preparation. D.C. provided the Can 10 cells, discussed the results and helped with manuscript preparation.

#### Funding

Work in the Bi laboratory is supported by the National Institutes of Health (NIH) [grant number GM87365] and a pilot grant from the University Research Foundation. Work in the Stanger laboratory is supported by the NIH [grant numbers DK083355 and DK083111] and the Pew Charitable Trusts. Deposited in PMC for release after 12 months.

#### Supplementary material

Supplementary material available online at
http://jcs.biologists.org/lookup/suppl/doi:10.1242/jcs.139923/-/DC1

#### References

**Akhmanova, A. and Steinmetz, M. O.** (2010). Microtubule +TIPs at a glance. *J. Cell Sci.* **123**, 3415-3419.

**Bartles, J. R. and Hubbard, A. L.** (1986). Preservation of hepatocyte plasma membrane domains during cell division in situ in regenerating rat liver. *Dev. Biol.* **118**, 286-295.

**Bi, E. and Park, H. O.** (2012). Cell polarization and cytokinesis in budding yeast. *Genetics* **191**, 347-387.

**Bretscher, A.** (2003). Polarized growth and organelle segregation in yeast: the tracks, motors, and receptors. *J. Cell Biol.* **160**, 811-816.
**Caviston, J. P. and Holzbaur, E. L.** (2006). Microtubule motors at the intersection of trafficking and transport. *Trends Cell Biol.* **16**, 530-537.
**Cohen, D., Brennwald, P. J., Rodriguez-Boulan, E. and Müsch, A.** (2004). Mammalian PAR-1 determines epithelial lumen polarity by organizing the microtubule cytoskeleton. *J. Cell Biol.* **164**, 717-727.
**Datta, A., Bryant, D. M. and Mostov, K. E.** (2011). Molecular regulation of lumen morphogenesis. *Curr. Biol.* **21**, R126-R136.
**Decaens, C., Durand, M., Grosse, B. and Cassio, D.** (2008). Which in vitro models could be best used to study hepatocyte polarity? *Biol. Cell* **100**, 387-398.
**Delacour-Larose, M., Molla, A., Skoufias, D. A., Margolis, R. L. and Dimitrov, S.** (2004). Distinct dynamics of Aurora B and Survivin during mitosis. *Cell Cycle* **3**, 1418-1426.
**Feldman, J. L. and Priess, J. R.** (2012). A role for the centrosome and PAR-3 in the hand-off of MTOC function during epithelial polarization. *Curr. Biol.* **22**, 575-582.
**Fleming, E. S., Zajac, M., Moschenross, D. M., Montrose, D. C., Rosenberg, D. W., Cowan, A. E. and Tirnauer, J. S.** (2007). Planar spindle orientation and asymmetric cytokinesis in the mouse small intestine. *J. Histochem. Cytochem.* **55**, 1173-1180.
**Founounou, N., Loyer, N. and Le Borgne, R.** (2013). Septins regulate the contractility of the actomyosin ring to enable adherens junction remodeling during cytokinesis of epithelial cells. *Dev. Cell* **24**, 242-255.
**Fu, D., Wakabayashi, Y., Ido, Y., Lippincott-Schwartz, J. and Arias, I. M.** (2010). Regulation of bile canalicular network formation and maintenance by AMP-activated protein kinase and LKB1. *J. Cell Sci.* **123**, 3294-3302.
**Fu, D., Wakabayashi, Y., Lippincott-Schwartz, J. and Arias, I. M.** (2011). Bile acid stimulates hepatocyte polarization through a cAMP-Epac-MEK-LKB1-AMPK pathway. *Proc. Natl. Acad. Sci. USA* **108**, 1403-1408.
**Gonzalez-Mariscal, L., Chávez de Ramírez, B. and Cereijido, M.** (1985). Tight junction formation in cultured epithelial cells (MDCK). *J. Membr. Biol.* **86**, 113-125.
**Gromley, A., Yeaman, C., Rosa, J., Redick, S., Chen, C. T., Mirabelle, S., Guha, M., Sillibourne, J. and Doxsey, S. J.** (2005). Centriolin anchoring of exocyst and SNARE complexes at the midbody is required for secretory-vesicle-mediated abscission. *Cell* **123**, 75-87.
**Gruneberg, U., Neef, R., Honda, R., Nigg, E. A. and Barr, F. A.** (2004). Relocation of Aurora B from centromeres to the central spindle at the metaphase to anaphase transition requires MKlp2. *J. Cell Biol.* **166**, 167-172.
**Guillot, C. and Lecuit, T.** (2013). Adhesion disengagement uncouples intrinsic and extrinsic forces to drive cytokinesis in epithelial tissues. *Dev. Cell* **24**, 227-241.
**Hao, Y., Du, Q., Chen, X., Zheng, Z., Balsbaugh, J. L., Maitra, S., Shabanowitz, J., Hunt, D. F. and Macara, I. G.** (2010). Par3 controls epithelial spindle orientation by aPKC-mediated phosphorylation of apical Pins. *Curr. Biol.* **20**, 1809-1818.
**He, B. and Guo, W.** (2009). The exocyst complex in polarized exocytosis. *Curr. Opin. Cell Biol.* **21**, 537-542.
**Helfrich, I., Schmitz, A., Zigrino, P., Michels, C., Haase, I., le Bivic, A., Leitges, M. and Niessen, C. M.** (2007). Role of aPKC isoforms and their binding partners Par3 and Par6 in epidermal barrier formation. *J. Invest. Dermatol.* **127**, 782-791.
**Herszterg, S., Leibfried, A., Bosveld, F., Martin, C. and Bellaiche, Y.** (2013). Interplay between the dividing cell and its neighbors regulates adherens junction formation during cytokinesis in epithelial tissue. *Dev. Cell* **24**, 256-270.
**Hirose, T., Izumi, Y., Nagashima, Y., Tamai-Nagai, Y., Kurihara, H., Sakai, T., Suzuki, Y., Yamanaka, T., Suzuki, A., Mizuno, K. et al.** (2002). Involvement of ASIP/PAR-3 in the promotion of epithelial tight junction formation. *J. Cell Sci.* **115**, 2485-2495.
**Hogan, B. L. and Kolodziej, P. A.** (2002). Organogenesis: molecular mechanisms of tubulogenesis. *Nat. Rev. Genet.* **3**, 513-523.
**Ishii, M., Washioka, H., Tonosaki, A. and Toyota, T.** (1991). Regional orientation of actin filaments in the pericanalicular cytoplasm of rat hepatocytes. *Gastroenterology* **101**, 1663-1672.
**Jaffe, A. B., Kaji, N., Durgan, J. and Hall, A.** (2008). Cdc42 controls spindle orientation to position the apical surface during epithelial morphogenesis. *J. Cell Biol.* **183**, 625-633.
**Kung, J. W., Currie, I. S., Forbes, S. J. and Ross, J. A.** (2010). Liver development, regeneration, and carcinogenesis. *J. Biomed. Biotechnol.* **2010**, 984248.
**Lázaro-Diéguez, F., Cohen, D., Fernandez, D., Hodgson, L., van Ijzendoorn, S. C. and Müsch, A.** (2013). Par1b links lumen polarity with LGN-NuMA positioning for distinct epithelial cell division phenotypes. *J. Cell Biol.* **203**, 251-264.
**Lubarsky, B. and Krasnow, M. A.** (2003). Tube morphogenesis: making and shaping biological tubes. *Cell* **112**, 19-28.
**Maddox, A. S., Lewellyn, L., Desai, A. and Oegema, K.** (2007). Anillin and the septins promote asymmetric ingression of the cytokinetic furrow. *Dev. Cell* **12**, 827-835.
**Martin, S. G. and Chang, F.** (2005). New end take off: regulating cell polarity during the fission yeast cell cycle. *Cell Cycle* **4**, 1046-1049.
**Martin-Belmonte, F. and Mostov, K.** (2008). Regulation of cell polarity during epithelial morphogenesis. *Curr. Opin. Cell Biol.* **20**, 227-234.
**McCaffrey, L. M. and Macara, I. G.** (2012). Signaling pathways in cell polarity. *Cold Spring Harb. Perspect. Biol.* **4**, a009654.
**McNeil, E., Capaldo, C. T. and Macara, I. G.** (2006). Zonula occludens-1 function in the assembly of tight junctions in Madin-Darby canine kidney epithelial cells. *Mol. Biol. Cell* **17**, 1922-1932.
**Murata-Hori, M., Tatsuka, M. and Wang, Y. L.** (2002). Probing the dynamics and functions of aurora B kinase in living cells during mitosis and cytokinesis. *Mol. Biol. Cell* **13**, 1099-1108.
**Navarro-Alvarez, N., Soto-Gutierrez, A. and Kobayashi, N.** (2010). Hepatic stem cells and liver development. *Methods Mol. Biol.* **640**, 181-236.
**Novick, P. and Guo, W.** (2002). Ras family therapy: Rab, Rho and Ral talk to the exocyst. *Trends Cell Biol.* **12**, 247-249.
**Peng, X., Grosse, B., Le Tiec, B., Nicolas, V., Delagebeaudeuf, C., Bedda, T., Decaens, C. and Cassio, D.** (2006). How to induce non-polarized cells of hepatic origin to express typical hepatocyte polarity: generation of new highly polarized cell models with developed and functional bile canaliculi. *Cell Tissue Res.* **323**, 233-243.
**Pollarolo, G., Schulz, J. G., Munck, S. and Dotti, C. G.** (2011). Cytokinesis remnants define first neuronal asymmetry in vivo. *Nat. Neurosci.* **14**, 1525-1533.
**Rodríguez-Fraticelli, A. E., Gálvez-Santisteban, M. and Martín-Belmonte, F.** (2011). Divide and polarize: recent advances in the molecular mechanism regulating epithelial tubulogenesis. *Curr. Opin. Cell Biol.* **23**, 638-646.
**Rodríguez-Fraticelli, A. E., Auzan, M., Alonso, M. A., Bornens, M. and Martín-Belmonte, F.** (2012). Cell confinement controls centrosome positioning and lumen initiation during epithelial morphogenesis. *J. Cell Biol.* **198**, 1011-1023.
**Schindelin, J., Arganda-Carreras, I., Frise, E., Kaynig, V., Longair, M., Pietzsch, T., Preibisch, S., Rueden, C., Saalfeld, S., Schmid, B. et al.** (2012). Fiji: an open-source platform for biological-image analysis. *Nat. Methods* **9**, 676-682.
**Schlüter, M. A., Pfarr, C. S., Pieczynski, J., Whiteman, E. L., Hurd, T. W., Fan, S., Liu, C. J. and Margolis, B.** (2009). Trafficking of Crumbs3 during cytokinesis is crucial for lumen formation. *Mol. Biol. Cell* **20**, 4652-4663.
**Slim, C. L., Lázaro-Diéguez, F., Bijlard, M., Toussaint, M. J., de Bruin, A., Du, Q., Müsch, A. and van Ijzendoorn, S. C.** (2013). Par1b induces asymmetric inheritance of plasma membrane domains via LGN-dependent mitotic spindle orientation in proliferating hepatocytes. *PLoS Biol.* **11**, e1001739.
**St Johnston, D. and Ahringer, J.** (2010). Cell polarity in eggs and epithelia: parallels and diversity. *Cell* **141**, 757-774.
**Streiblova, E., Beran, K. and Pokorny, V.** (1964). Multiple scars, a new type of yeast scar in apiculate yeasts. *J. Bacteriol.* **88**, 1104-1111.
**Tawk, M., Araya, C., Lyons, D. A., Reugels, A. M., Girdler, G. C., Bayley, P. R., Hyde, D. R., Tada, M. and Clarke, J. D.** (2007). A mirror-symmetric cell division that orchestrates neuroepithelial morphogenesis. *Nature* **446**, 797-800.
**Tirnauer, J. S. and Bierer, B. E.** (2000). EB1 proteins regulate microtubule dynamics, cell polarity, and chromosome stability. *J. Cell Biol.* **149**, 761-766.
**Treyer, A. and Müsch, A.** (2013). Hepatocyte polarity. *Compr. Physiol.* **3**, 243-287.
**Tsukada, N., Ackerley, C. A. and Phillips, M. J.** (1995). The structure and organization of the bile canalicular cytoskeleton with special reference to actin and actin-binding proteins. *Hepatology* **21**, 1106-1113.
**Tuma, P. L., Finnegan, C. M., Yi, J. H. and Hubbard, A. L.** (1999). Evidence for apical endocytosis in polarized hepatic cells: phosphoinositide 3-kinase inhibitors lead to the lysosomal accumulation of resident apical plasma membrane proteins. *J. Cell Biol.* **145**, 1089-1102.
**Tuma, P. L., Nyasae, L. K., Backer, J. M. and Hubbard, A. L.** (2001). Vps34p differentially regulates endocytosis from the apical and basolateral domains in polarized hepatic cells. *J. Cell Biol.* **154**, 1197-1208.
**Wakabayashi, Y., Dutt, P., Lippincott-Schwartz, J. and Arias, I. M.** (2005). Rab11a and myosin Vb are required for bile canalicular formation in WIF-B9 cells. *Proc. Natl. Acad. Sci. USA* **102**, 15087-15092.
**Wang, L. and Boyer, J. L.** (2004). The maintenance and generation of membrane polarity in hepatocytes. *Hepatology* **39**, 892-899.
**Wood, R. L.** (1965). An electron microscope study of developing bile canaliculi in the rat. *Anat. Rec.* **151**, 507-529.
**Zegers, M. M. and Hoekstra, D.** (1998). Mechanisms and functional features of polarized membrane traffic in epithelial and hepatic cells. *Biochem. J.* **336**, 257-269.

## Supplementary materials

## Supplementary figure legends

**Fig. S1. Knockdown of Par3 prevents *de novo* BC formation and tubular BC extension**
(**A**) Representative images of BC formation in the control (si Con) and Par3-knockdown (si Par3) cells. Mdr, green; DNA, green. Scale bar, 10 μm. (**B**) The percentage of cells engaged in BC formation is 61 ± 6% (SD) for siPar3 cells (n = 12 image fields; total 837 cells quantified) compared to control cells (84 ± 3%; n = 8 image fields; total 786 cells quantified) ($p < 0.001$). (**C**) The BC lengths for the siCon (223 BCs for 786 cells quantified) and siPar3 (161 BCs for 837 cells quantified) cells are 15 ± 14 μm, and 8 ± 3 μm, respectively ($p < 0.001$). (**D**) Western blotting indicates that the level of Par3 (relative molecular mass: 150 kD) in the si Par3 cells was reduced to 11% of that in the control cells. Actin was used as a loading control. (**E-F**) Knockdown of Par3 does not appear to affect the maintenance of BC (**E**) or tight junction (**F**). Scale bars, 3 μm. The siRNA against Par3 used in this experiment (AGAGUUGGAUGACAGAGAACGCAGG, sense) was purchased from IDT, and the one used in Figure 4 (GGAGUAGAUUUAGCGGGCA, sense) was purchased from Invitrogen.

**Fig. S2. Distinct effects of LatA and NZ treatments on the actin cytoskeleton (F-actin, red), microtubules (tubulin, green), and BC architecture (ZO-1, blue), Related to Fig. 6A**
The separate image panels for the same cells presented in Fig. 6A (merged panel only) are shown here for clear visualization of the drug-treatment effects.

**Fig. S3. LatA treatment affects BC architecture (Mdr, red), Related to Fig. 6A**
Four representatives of the misshaped (cell pairs 1 and 2) and fragmented (cell pairs 3 and 4) BCs caused by LatA treatment. Scale bar, 3 μm.

**Fig. S4. Centrosome location (centriolin, green) during different stages of BC formation (ZO-1, red), Related to Fig. 6F**
During pre-BC stage, the centrosomes are either away from (cell pair 1) or near (cell pair 2) the BC membrane. However, during the small- and large-BC stages (cell pairs 3 and 4), the centrosomes are invariably close to the BC membrane. Scale bar, 3 μm.

**Supplementary movie Legends**

**Movie 1. BC formation is spatially linked to cytokinesis, Related to Fig. 1A**
A time-lapse movie showing a single BC-like structure at the cell division site two hours after cytokinesis. The BC was enlarged over time. Individual frames were acquired every four minutes.

**Movie 2. A time-lapse movie showing three cells undergoing cytokinesis and BC formation, Related to Fig. 1B**
At the end of this time-lapse analysis, the same three cells were fixed and stained for Mdr (green) to visualize BC formation at the division site. Individual frames were acquired every six minutes.

**Movie 3. Endocytosis of a BC structure, Related to Fig. 1**
A time-lapse movie showing endocytosis of a BC structure at the division site. Individual frames were acquired every four minutes.

**Movie 4. 3D reconstruction of the complex tight junction at the 3-cell stage, Related to Fig. 3D**
Tight-junction morphology (ZO-1, red) at the midbody stage (Aurora B, green) of second round of division was reconstructed in 3D using 0.3 μm × 21 optical sections.

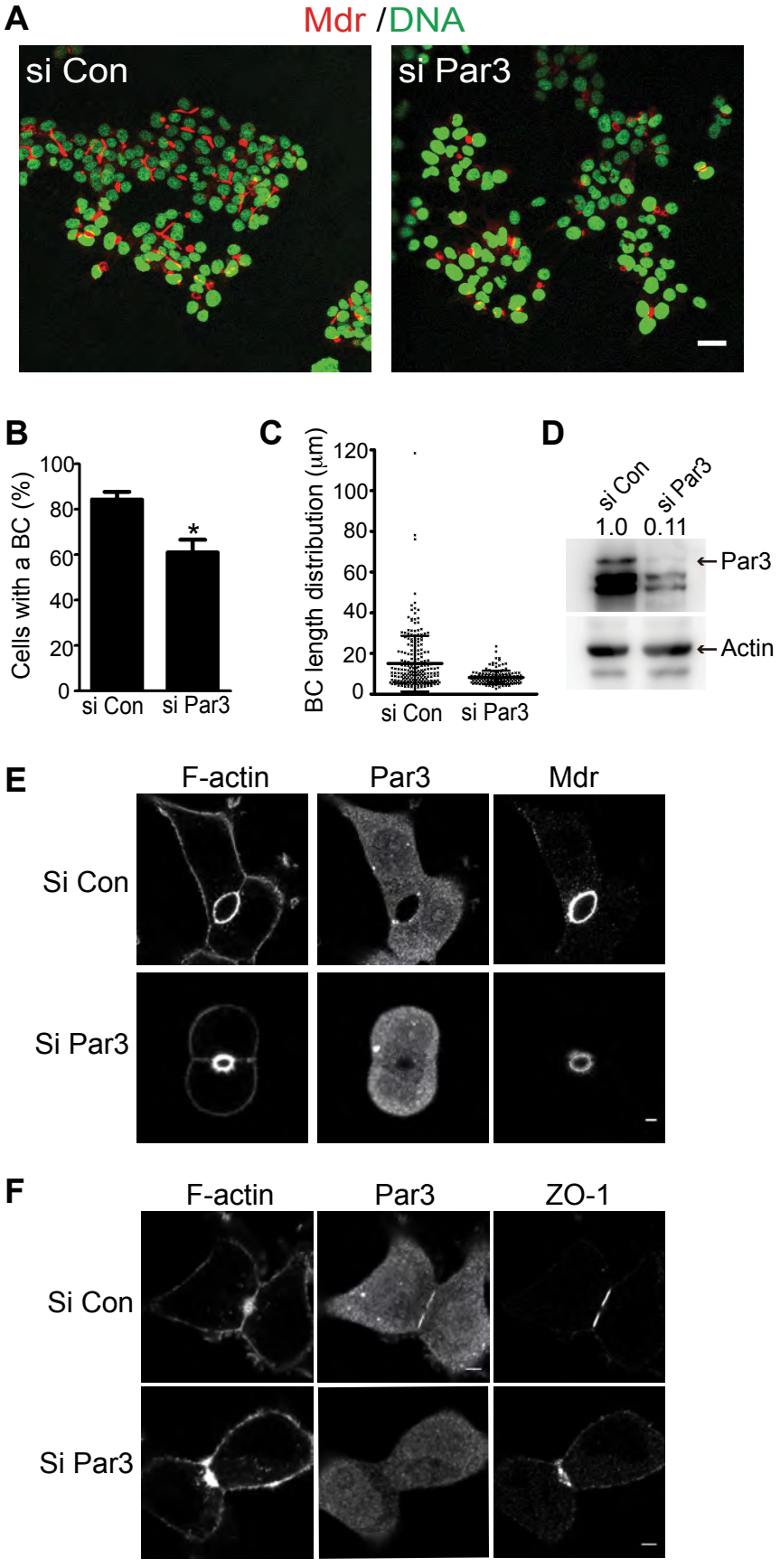


**Figure S1. Wang et al.**

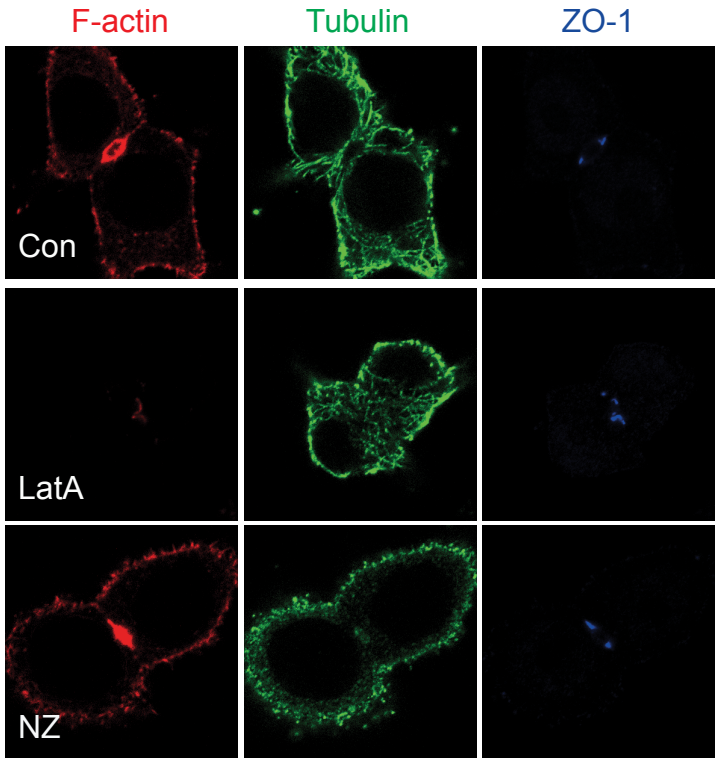


**Figure S2. Wang et al.**

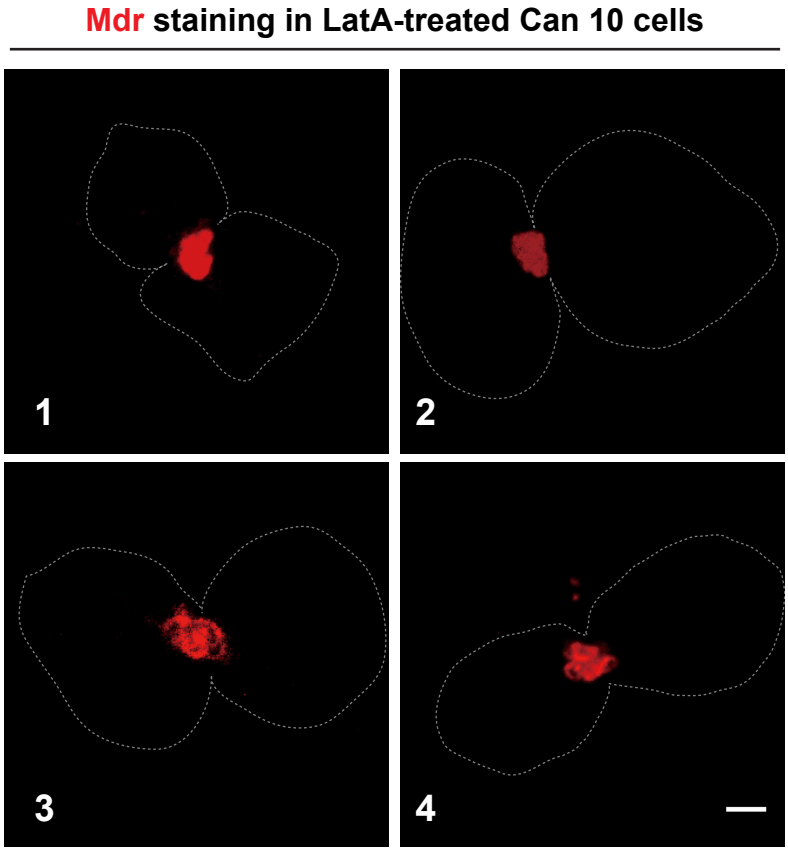


**Figure S3. Wang et al.**

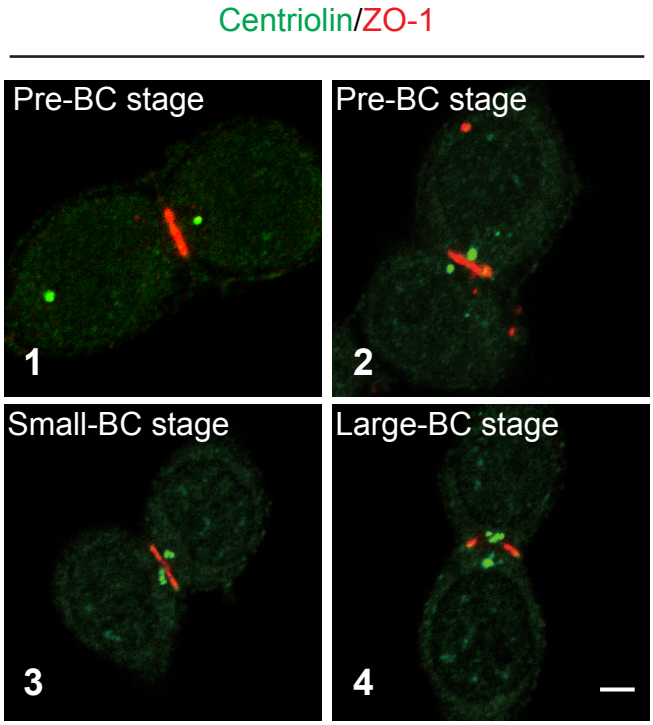


**Figure S4. Wang et al.**


**Movie 1.**

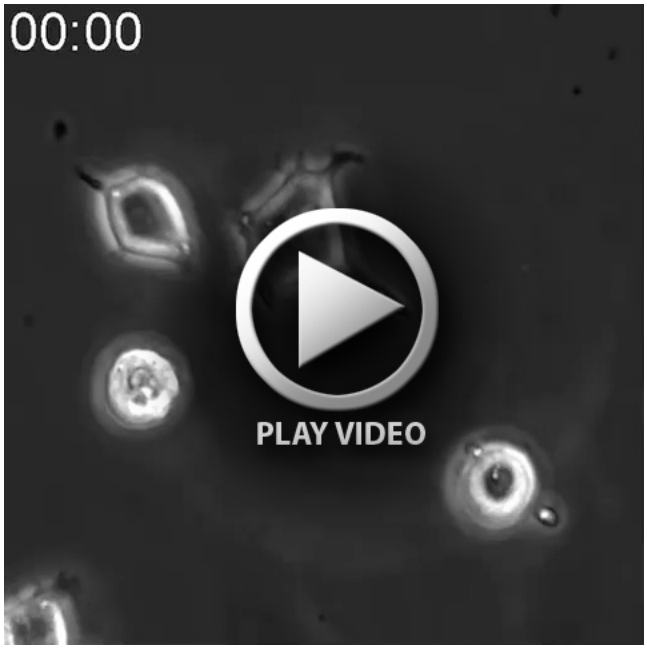


**Movie 2.**


**Movie 3.**


**Movie 4**